Development of Small-Molecule Cyclin D1-Ablative Agents

Jui-Wen Huang,[†] Chung-Wai Shiau,[†] Jian Yang,[†] Da-Sheng Wang,[†] Hao-Chieh Chiu,[†] Ching-Yu Chen,[‡] and Ching-Shih Chen*[,†]

Division of Medicinal Chemistry and Pharmacognosy, College of Pharmacy, 336 Parks Hall, The Ohio State University, 500 West 12th Avenue, Columbus, Ohio 43210, Department of Family Medicine, College of Medicine, National Taiwan University, Taipei, Taiwan, and The Division of Gerontology Research, National Health Research Institutes, Taipei, Taiwan

Received January 17, 2006

Previously, we demonstrated that the peroxisome proliferator-activated receptor γ (PPARγ) agonist troglitazone mediated the repression of cyclin D1 in MCF-7 breast cancer cells by facilitating proteasome-facilitated proteolysis. This PPARγ-independent mechanism provided a molecular basis for using troglitazone as scaffold to develop a novel class of cyclin D1-ablative agents. The proof of principle of this premise is provided by Δ2TG, in which the introduction of a double bond adjacent to the thiazolidinedione ring abrogated the PPARγ activity while retaining the activity in cyclin D1 repression. Structural optimization of Δ2TG led to STG28 [(*S*)-5-(4-{[6-(allyloxy)-2,5,7,8-tetramethylchroman-2-yl]methoxy}-3-methoxybenzylidene)-thiazolidine-2,4-dione], which exhibited low micromolar potency in ablating cyclin D1 and inhibiting MCF-7 cell proliferation. It is noteworthy that STG28 mediated the proteasomal degradation of cyclin D1 with a high degree of specificity. Exposure to STG28 did not cause any appreciable change in the expression levels of a series of other cyclins and CDK-dependent kinases. In light of the pivotal role of cyclin D1 in promoting tumorigenesis and drug resistance, this novel cyclin D1-ablating agent may have therapeutic relevance in cancer therapy.

Introduction

Overexpression of the cell cycle control gene cyclin D1 represents a key mechanism underlying tumorigenesis, tumor progression, and metastasis in a variety of human cancers.[1−6] Evidence indicates that cyclin D1 regulates cell cycle progression and proliferation through the interaction with multiple signaling targets.[5,6] Cyclin D1 serves as the regulatory subunit of cyclin-dependent kinases (CDKs) 4 and 6 and exhibits the ability to bind and sequester the CDK inhibitor p27.[5,6] Together, these functions facilitate CDK-mediated inactivating phosphorylation of the retinoblastoma protein (pRb), resulting in G1/S progression. In addition, this cell cycle regulator may regulate transcription through physical associations with a plethora of transcriptional factors, coactivators, and corepressors that govern histone acetylation and chromatin remodeling proteins.[6] The concerted action of these CDK-dependent and CDK-independent functions underscores the oncogenic potential of cyclin D1 in many forms of cancer.[7] Inhibition of cyclin D1 expression by antisense oligonucleotides has been shown to block tumorigenesis or to reverse the transformed phenotype of human esophageal,[8] lung,[9] colon,[10] pancreatic,[11] gastric,[12,13] melanoma,[14] and squamous cancer cells[15] in mice.

In light of the function of cyclin D1 as an oncogene, targeting its expression represents a promising strategy for cancer therapy.[16] Cyclin D1 is induced by a multitude of proliferative and transforming signaling pathways, including the RAS/RAF/ERK, PI3K/PDK-1, WNT/β-catenin, and PKA/CREB pathways, and undergoes rapid proteasomal degradation upon the withdrawal of growth factors.[5,6] Previously, we reported that the peroxisome proliferator-activated receptor γ (PPARγ) agonist troglitazone, at high doses, facilitated the proteasomal proteolysis of cyclin D1 independently of PPARγ.[17] The dissociation of these two pharmacological activities, i.e., cyclin D1 repression versus PPARγ activation, provides a molecular basis for using troglitazone as scaffold to develop novel agents with high potency in repressing cyclin D1 expression. This structural optimization has led to a novel class of cyclin D1-ablative agents with low-micromolar potency.

Chemistry

In our previous report, we demonstrated that introduction of a double bond adjoining the terminal thiazolidine-2,4-dione ring of troglitazone abrogated the PPARγ agonist activity without compromising the cyclin D1-repressing activity.[17] Thus, the resulting PPAR-γ-inactive analogue Δ2TG (Figure 1A) was used as a lead compound in this study for structural modifications. To envisage the role of the vitamin E antioxidant moiety in the effect of Δ2TG on cyclin D1 ablation, different substituents were added to the terminal hydroxyl function of Δ2TG, yielding compounds **1**−**5**. Among them, addition of an allyl, 3,3-dimethylallyl, or benzyl group to Δ2TG resulted in a multifold increase in the cyclin D1-ablating activity. Subsequently, compound **6** was synthesized to examine the effect of the orientation of the thiazolidinedione ring on the activity. Furthermore, we used the allyl- and 3,3-dimethylallyl-substituted analogues of Δ2TG as platforms to carry out structural optimization, which generated two series of compounds, i.e., **7**−**10** and **11**−**16**, respectively. These Δ2TG derivatives were synthesized according to a general procedure described in Figure 1B. All derivatives synthesized, including Δ2TG, were racemic compounds unless otherwise indicated.

Results

Pharmacological Exploitation of PPARγ-Independent Effect of Troglitazone on Cyclin D1 Repression To Generate a Novel Class of Cyclin D1-Ablative Agents. Dose-dependent effect of troglitazone and Δ2TG on cyclin D1 repression in MCF-7 cells was examined by Western blot analysis after 72 h of drug treatment (Figure 2A). Δ2TG, though devoid of PPARγ agonist activity, exhibited slightly higher potency in repressing

* To whom correspondence should be addressed. Phone: (614) 688-4008. Fax: (614) 688-8556. E-mail: chen.844@osu.edu.
[†] The Ohio State University.
[‡] National Taiwan University and National Health Research Institutes.

10.1021/jm060057h CCC: $33.50
Published on Web 06/29/2006

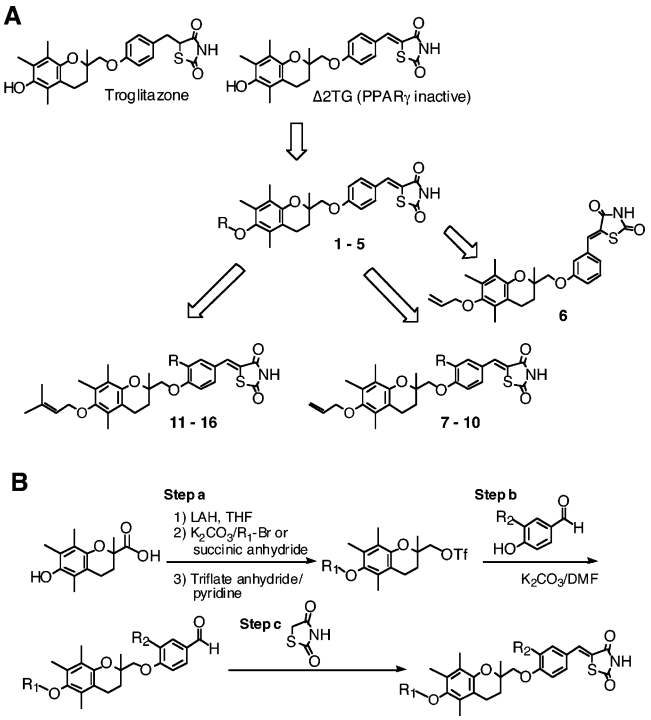

Figure 1. (A) Representative structures of troglitazone and derivatives and (B) the general synthetic procedure for troglitazone derivatives.

cyclin D1 compared to troglitazone. For example, the concentration required for the complete abrogation of cyclin D1 expression was approximately 30 μM for Δ2TG vis-à-vis 40 μM for troglitazone. Earlier, we have demonstrated that this troglitazone- and Δ2TG-mediated cyclin D1 down-regulation was caused by ubiquitin-dependent proteasomal degradation.[17] Together, these findings suggest that the effect of these agents on cyclin D1 repression was independent of PPARγ activation. Consequently, Δ2TG was used as a starting point for structural optimization to generate cyclin D1-ablative agents with low-micromolar potency.

Lead Optimization: Steric and Stereochemical Effects. Δ2TG was first conjugated with different substituents through an ether linkage at the terminal hydroxyl function, generating compounds **1**−**5**. These derivatives were analyzed by Western blotting for their ability, within the dose range of 2.5−7.5 μM, to repress cyclin D1 expression in MCF-7 cells (Figure 2B). Among the five derivatives examined, the allyl (**1**), 3,3-dimethylallyl (**2**), and benzyl (**3**) derivatives gave robust reduction in cyclin D1 levels at concentrations below 5 μM after 72 h of exposure, while the cinnamyl (**4**) and succinyl (**5**) counterparts had only moderate effect even at 7.5 μM. This differential increase in potency suggests a unique mode of ligand recognition that preferred less bulky hydrophobic side chains. The 4- to 5-fold improvement in the cyclin D1-ablating activity of compounds **1**−**3** over Δ2TG indicates the importance of this hydrophobic interaction in ligand binding.

Our data also suggest the requirement of a linear, elongated ligand structure for the high potency in cyclin D1 ablation. For example, changing the relative position of the terminal methylene-2,4-thiazolidinedione moiety to the phenyl ring from para to meta (**1** → **6**) substantially attenuated the cyclin D1-repressing potency (Figure 2B).

With **1** and **2** as lead compounds, we further examined the effect of modifying the benzylidene moiety with different substitutions on cyclin D1-ablating activity. Among the four different analogues of **1** examined, the methoxy derivative (**8**)

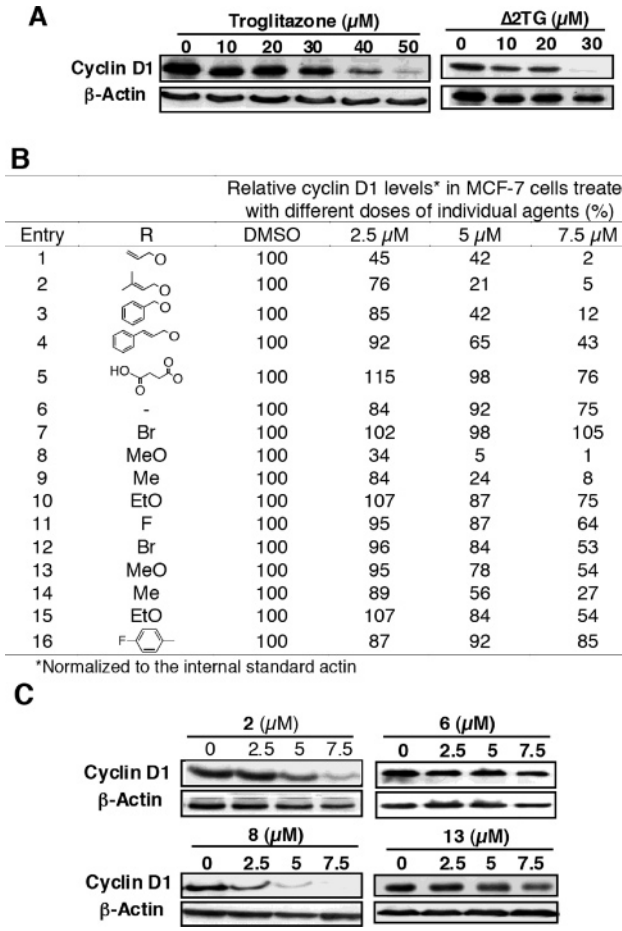

Relative cyclin D1 levels* in MCF-7 cells treated with different doses of individual agents (%)

Entry	R	DMSO	2.5 μM	5 μM	7.5 μM
1		100	45	42	2
2		100	76	21	5
3		100	85	42	12
4		100	92	65	43
5		100	115	98	76
6	-	100	84	92	75
7	Br	100	102	98	105
8	MeO	100	34	5	1
9	Me	100	84	24	8
10	EtO	100	107	87	75
11	F	100	95	87	64
12	Br	100	96	84	53
13	MeO	100	95	78	54
14	Me	100	89	56	27
15	EtO	100	107	84	54
16		100	87	92	85

*Normalized to the internal standard actin

Figure 2. Dose-dependent effect of troglitazone, Δ2TG, and compounds **1**−**16** on cyclin D1 ablation in MCF-7 breast cancer cells. MCF-7 cells were exposed to the individual agents at the indicated concentrations in 5% FBS-supplemented medium for 72 h, and the expression of cyclin D1 was analyzed by Western blot analysis with β-actin as an internal standard: (A) Western blot analysis of the dose-dependent effect of troglitazone and Δ2TG on cyclin D1 repression; (B) a summary of the differential effect of compounds **1**−**16** on cyclin D1 ablation. The general structures for these compounds are shown in Figure 1. Intensities of cyclin D1 immunostaining in Western blots were measured by densitometry and after being normalized to that of actin were presented as numerical data with the DMSO control as 100%. (C) Representative Western blotting of compounds **2**, **6**, **8**, and **13** is shown at the indicated concentrations.

exhibited the highest potency with multifold improvement over the parent compound, followed by the methyl derivative (**9**), while the bromo and methyoxy counterparts (**7** and **10**, respectively) showed modest or no appreciable reduction in cyclin D1-ablating activity (Figure 2B). The IC_{50} of **8** in mediating the repression of cyclin D1 was approximately 2.5 μM after 72 h of exposure, compared to greater than 5 μM for **1**. On the other hand, derivatization of **2** with various functional groups (compounds **11**−**16**) led to a decrease in potency irrespective of the size and stereoelectronic property of these substituents (Figure 2B).

In light of the high potency of **8**, we further compared the activity of its optically active isomers. Figure 3 depicts the dose-dependent effect of (*S*)-**8** (left panel, named STG28 from this point on) and (*R*)-**8** (right panel) in repressing the expression of cyclin D1 in MCF-7 cells after a 24-h treatment. These data clearly indicate a stereochemical preference in the pharmacological action, i.e., the potency of the (*S*)-isomer was severalfold higher than that of the (*R*)-counterpart. In line with its enhanced ability in cyclin D1 ablation, STG28 exhibited significantly

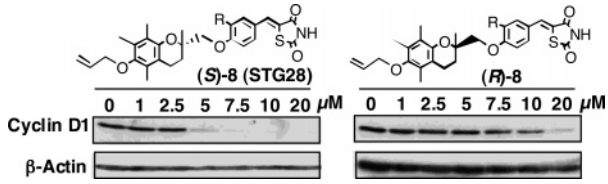

Figure 3. Dose-dependent effect of (*S*)-**8** (STG28) versus (*R*)-**8** on cyclin D1 ablation. MCF-7 cells were exposed to the individual agents at the indicated concentrations in 5% FBS-supplemented medium for 24 h, and the expression of cyclin D1 was analyzed by Western blot analysis with β-actin as an internal standard.

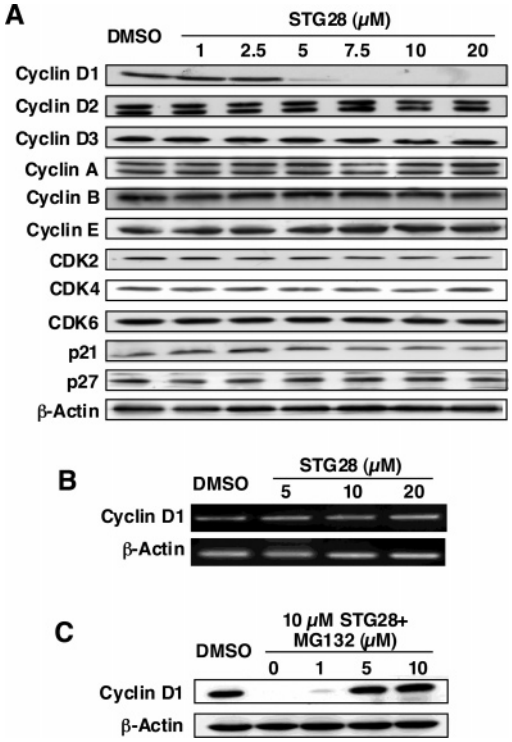

Figure 4. Mechanistic validation of the mode of action of STG28. (A) Effect of STG28 on cyclin D1 ablation is highly specific. MCF-7 cells were exposed to STG28 at the indicated concentrations in 5% FBS-supplemented medium for 24 h, and the expression of various cyclins, CDKs, the CDK inhibitors p21 and p27 was analyzed by Western blot analysis with β-actin as an internal standard. (B) STG28-facilitated cyclin D1 ablation is mediated at the post-transcriptional level. Drug-treated MCF-7 cells were subjected to total RNA isolation, followed by RT-PCR analysis of mRNA transcripts of cyclin D1 gene, as described in the Experimental Section. (C) STG28-facilitated cyclin D1 ablation is mediated through proteasomal degradation. MCF-7 cells were exposed to 10 μM STG28 in the presence of various concentrations of the proteasome inhibitor MG132 in 5% FBS-supplemented medium for 24 h, and the expression of cyclin D1 was analyzed by Western blot analysis with β-actin as an internal standard.

higher potency than Δ2TG in inhibiting MCF-7 cell proliferation (IC_{50} of 5 vs 55 μM).

Mechanistic Validation of the Mode of Action of STG28. Previously, we demonstrated that troglitazone and Δ2TG facilitated proteasomal degradation of cyclin D1 in a highly specific manner.[17] Here, we carried out the following three experiments to validate the mechanism by which STG28 mediated cyclin D1 ablation. First, to demonstrate that the ablative effect of STG28 was unique to cyclin D1, we assessed the expression levels of cyclins D2, D3, A, B, and E, CDKs 2 and 4, and the CDK inhibitors p21 and p27 in MCF-7 cells exposed to different doses of STG28 for 24 h (Figure 4A). As shown, with the exception of a slight decrease in p21 levels, no appreciable change was noted in the expression level of these

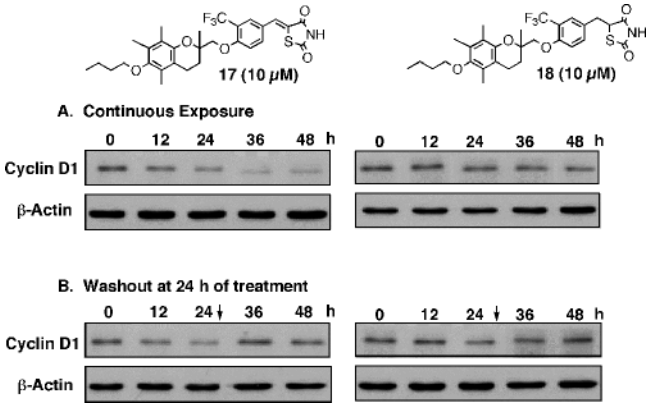

Figure 5. Evidence that the effect of unsaturated thiazolidinedione derivatives on cyclin D1 repression is reversible. The effect of the unsaturated thiazolidinedione **17** vis-à-vis its saturated counterpart **18**, each at 10 μM, on cyclin D1 repression in MCF-7 cells was examined at different intervals throughout a 48 h period in two different manners. (A) For continuous exposure, cells in T-75 flasks were incubated in drug-containing, 5% FBS-supplemented medium for 48 h. (B) For washout at 24 h of treatment, cells in T-75 flasks were exposed to the agent for 24 h, followed by incubation in drug-free medium for an additional 24 h. Cyclin D1 levels in cell lysates were analyzed by Western blot analysis with β-actin as an internal standard.

cell cycle-regulatory proteins, underscoring the high degree of specificity in the effect of STG28 on cyclin D1 repression.

Second, semiquantitative PCR (polymerase chain reaction) showed that the mRNA level of cyclin D1 remained unaltered after 24 h of exposure to different doses of STG28 (Figure 4B), indicating that the repression occurred at the protein level.

Third, we tested the effect of the proteasome inhibitor MG132 on the protection of STG28-mediated cyclin D1 ablation (Figure 4C). As shown, MG132 at 5 and 10 μM was effective in rescuing the drug-induced cyclin D1 repression, providing a mechanistic link with proteasome-mediated proteolysis.

Together, these findings confirmed that STG28 mediated the repression of cyclin D1 through the same mode of mechanism as that of troglitazone and Δ2TG. The target that these Δ2TG derivatives use to facilitate proteasomal degradation of cyclin D1 remains unclear. However, the presence of the benzylidine-thiazolidine-2,4-dione substructure raised a possibility that these Δ2TG derivatives might act as "Michael acceptors" by covalently modifying the target enzyme/protein upon binding. To examine this possibility, we assessed the effect of an unsaturated thiazolidinedione (**17**) vis-à-vis its saturated counterpart (**18**) on cyclin D1 ablation by using a washout experiment. Compounds **17** and **18** exhibited IC_{50} of 6 and 9 μM, of which the relative ratio was in line with that of Δ2TG to troglitazone. Figure 5A shows the time-dependent effect of **17** (left panel) and **18** (right panel), each at 10 μM, on the suppression of cyclin D1 expression. In a parallel experiment in which these agents were washed out from the medium after 24 h of exposure, the cyclin D1 level rapidly returned to normal regardless of the unsaturated thiazolidinedione moiety (Figure 5B). These data suggest a reversible nature of this ligand−protein interaction.

Discussion

On the basis of the mechanistic finding that the effect of troglitazone on cyclin D1 repression was independent of PPARγ activation,[17] this study embarked on the structural optimization of troglitazone to develop a novel class of cyclin D1-ablative agents. Our premise that troglitazone's pharmacological activities in cyclin D1 ablation and PPARγ activation could be structurally dissociated was borne out by Δ2TG, which, albeit

devoid of PPARγ activity, exhibited a slightly higher cyclin D1-ablating activity. Presumably, the rigid, liner substructure of benzylidene-thiazolidinedione of Δ2TG prohibited its interaction with PPARγ. Subsequent modifications of Δ2TG by adding hydrophobic side chains, including allyl, dimethylallyl, and benzyl, to the terminal hydroxyl function (compounds **1**, **2**, and **3**, respectively) resulted in a multifold increase in cyclin D1-repressing potency. This increase, however, was not noted with an extended aromatic side chain such as cinnamyl (**4**) or a charged group such as succinyl (**5**). Moreover, the requirement of a linear structure for the ligand recognition was underscored by the substantially lower potency of **6** compared to **1**. Further modifications of the benzylidene moiety in **1** and **2** revealed a subtle effect of the 3-substitution on cyclin D1 ablation. Among the 10 derivatives examined (**7**−**16**), **8** showed the highest activity, followed by **9**, while the other derivatives displayed decreased potency. It is also noteworthy that the ability of **8** in cyclin D1 repression was stereospecific; i.e., the (*S*)-enantiomer (STG28) was more active than the (*R*)-counterpart. STG28 was able to repress cyclin D1 at low-micromolar concentrations, while (*R*)-**8** required at least 10 μM to achieve the same extent of repression.

Equally important, STG28-mediated cyclin D1 ablation was highly specific. Our data indicate that none of the other cyclins examined were affected by STG28. The mode of action of STG28 in facilitating cyclin D1 ablation was identical to that of its parent compound, i.e., via proteasome-mediated proteolysis. From a mechanistic perspective, STG28 provides a useful pharmacological tool to study the ubiquitin-dependent proteasomal degradation of cyclin D1, which constitutes the focus of our current investigation.

Conclusion

STG28 represents the first small-molecule agent that exhibits high potency in repressing cyclin D1 expression. This agent may have therapeutic relevance in light of the pivotal role of cyclin D1 in promoting tumorigenesis and drug resistance. In breast cancer, overexpression of this cell cycle regulator confers resistance to antiestrogens and represents a negative predictive factor for tamoxifen response. Thus, these findings underscore the potential use of this anti-cyclin D1 therapy in the treatment of breast cancer. Testing of STG28 in an in vivo breast tumor model is currently under way.

Experimental Section

Chemical reagents and organic solvents were purchased from Aldrich unless otherwise mentioned. Nuclear magnetic resonance spectra (^{1}H NMR) were measured on a Bruker AC 300, Bruker DPX 300, or Bruker DRX 400 model spectrometer. Chemical shifts (δ) were reported in parts per million (ppm) relative to the TMS peak. Electrospray ionization (ESI) mass spectrometry analyses were performed with a Micromass QTOF electrospray mass spectrometer. Elemental analyses were performed by the Atlantic Microlab, Inc. (Norcross, GA).

Troglitazone and the proteasome inhibitor MG132 were purchased from Sigma-Aldrich (St. Louis, MO). Δ2TG was synthesized as previously described.[17] Mouse anti-cyclin D1 was purchased from Cell Signaling Technology Inc. (Beverly, MA). Rabbit antibodies against CDK2, CDK4, cyclin A, cyclin B, cyclin D2, cyclin D3, cyclin E, p21, p27 were purchased from Santa Cruz Biotechnology, Inc. (Santa Cruz, CA). Mouse monoclonal anti-actin was purchased from MP Biomedicals (Irvine, CA). MTT [3-(4,5-dimethylthiazol-2-yl)-2,5-diphenyl-2*H*-tetrazolium bromide] for cell viability assay was purchased form TCI America, Inc. (Portland, OR).

Compounds **1**−**18** were synthesized according to the general procedure described in Figure 1B, which is illustrated by the synthesis of **1**, described as follows.

(*Z*)-5-{4-[(6-Allyloxy-2,5,7,8-tetramethylchroman-2-yl)methoxy]-benzylidene}thiazolidine-2,4-dione (1). Step a. (1) To a stirring solution of 0.78 g of $LiAlH_4$ (20 mmol) in 10 mL of THF at 0 °C was added 5 g (20 mmol) of 6-hydroxy-2,5,7,8-tetramethylchroman-2-carboxylic acid (Sigma-Aldrich, St. Louis, MO) in 250 mL of THF dropwise over a period of 1 h. The solution was stirred at room temperature under nitrogen for another 6 h, and 4 mL of 0.25 N NaOH was added to quench the reaction. The mixture was stirred at room temperature for 1 h, filtered, and concentrated under reduced pressure. The resulting residue was purified by flash silica gel chromatography (ethyl acetate/hexane, 1:2) to afford 2-hydroxymethyl-2,5,7,8-tetramethylchroman-6-ol in 75% yield.

(2) A mixture of the above purified product (2 mmol), allyl bromide (2 mmol), and K_2CO_3 (3 mmol) in 10 mL of acetone was refluxed for 48 h, filtered, and concentrated. The resulting residue was purified by flash silica gel chromatography (ethyl acetate/hexanes, 1:5) to yield (6-allyloxy-2,5,7,8-tetramethylchroman-2-yl)methanol in 81% yield.

(3) Triflate anhydride (0.19 mL, 1.1 mmol) was added dropwise into the mixture of the above purified product (1 mmol), pyridine (1.2 mmol), and 5 mL of CH_2Cl_2 at 0 °C. The solution was stirred at 0 °C for 30 min and concentrated. The resulting residue was purified by flash silica gel chromatography (ethyl acetate/hexanes, 1:10), giving (6-allyloxy-2,5,7,8-tetramethylchroman-2-yl)methyl trifluoromethanesulfonate in 92% yield.

Step b. The purified triflate from step a (0.5 mmol) in 2 mL of DMF was treated with K_2CO_3 (0.5 mmol) in 10 mL of DMF at 0 °C for 30 min, followed by 4-hydroxybenzaldehyde (0.5 mL, 4.7 mmol). The mixture was stirred at room temperature overnight, poured into water to quench the reaction, extracted with ethyl acetate, and concentrated. The resulting residue was purified by flash silica gel chromatography (ethyl acetate/hexanes, 1:10), resulting in 4-[(6-allyloxy-2,5,7,8-tetramethylchroman-2-yl)methoxy]-benzaldehyde in 93% yield.

Step c. A mixture of the above purified aldehyde (0.3 mmol), 4-thiazolidinedione (0.6 mmol), and a catalytic amount of piperidine was refluxed in 5 mL of EtOH for 24 h and concentrated. The oil product was dissolved in ethyl acetate, poured into water, and acidified with acetic acid. The mixture was extracted with ethyl acetate and concentrated. The resulting residue was purified by flash silica gel chromatography (ethyl acetate/hexanes, 1:5), generating **1** in 71% yield: ^{1}H NMR ($CDCl_3$) δ 1.30 (s, 3H), 1.83−1.93 (m, 1H), 2.04−2.16 (m, 10H), 2.58 (t, J = 5.8 Hz, 2 H), 3.95 (d, J = 8.8 Hz, 1 H), 4.03 (d, J = 8.8 Hz, 1 H), 4.15 (d, J = 11.5 Hz, 2 H), 5.23 (d, J = 10.1 Hz, 1 H), 5.41 (d, J = 18.2 Hz, 1 H), 6.02−6.17 (m, 1 H), 7.10 (d, J = 9.8 Hz, 2 H), 7.48 (d, J = 9.8 Hz, 2 H), 7.79 (s, 1 H), 8.56 (s, 1 H); HRMS exact mass of $(M + Na)^+$, 502.1658 amu; observed mass of $(M + Na)^+$, 502.1685 amu. Anal. ($C_{27}H_{29}NO_5S$) C, H, N.

(*Z*)-5-(4-((2,5,7,8-Tetramethyl-6-(3-methylbut-2-enyloxy)chroman-2-yl)methoxy)benzylidene)thiazolidine-2,4-dione (2): ^{1}H NMR ($CDCl_3$) δ 1.40 (s, 3 H), 1.63 (s, 3 H), 1.69 (s, 3 H), 1.88−1.93 (m, 1 H), 2.04−2.18 (m, 10 H), 2.61 (t, J = 6.8, 2 H), 3.95 (d, J = 9.3 Hz, 1 H), 4.03 (d, J = 9.3 Hz, 1 H), 4.15 (d, J = 7.0, 2 H), 5.58 (t, J = 7.2, 1 H), 7.01 (d, J = 8.8 Hz, 2 H), 7.42 (d, J = 8.8 Hz, 2 H), 7.90 (s, 1 H), 8.84 (s, 1 H); HRMS exact mass of $(M + Na)^+$, 530.1971 amu; observed mass of $(M + Na)^+$, 530.1975 amu. Anal. ($C_{29}H_{33}NO_5S$) C, H, N.

(*Z*)-5-{4-[(6-Benzyloxy-2,5,7,8-tetramethylchroman-2-yl)-methoxy]-3-bromobenzylidene}thiazolidine-2,4-dione (3): ^{1}H NMR ($CDCl_3$) δ 1.42 (s, 3 H), 1.84−1.95 (m, 1 H), 2.04−2.20 (m, 10 H), 2.62 (t, J = 6.9 Hz, 2 H), 3.95 (d, J = 9.3, 1 H), 4.01 (d, J = 9.3 Hz, 1 H), 4.67 (s, 2 H), 7.01 (d, J = 8.9 Hz, 2 H), 7.35−7.50 (m, 7 H), 7.79 (s, 1 H), 8.69 (brs, 1 H); HRMS exact mass of $(M + Na)^+$, 552.1815 amu; observed mass of $(M + Na)^+$, 552.1839 amu. Anal. ($C_{31}H_{31}NO_5S$) C, H, N.

(*Z*)-5-{4-[(6-Cinnamyloxy-2,5,7,8-tetramethylchroman-2-yl)-methoxy]benzylidene}thiazolidine-2,4-dione (4): ^{1}H NMR ($CDCl_3$) δ 1.41 (s, 3 H), 1.83−1.94 (m, 1 H), 2.02−2.20 (m, 10 H), 2.62 (t, J = 6.0 Hz, 2 H), 3.95 (d, J = 8.9 Hz, 1 H), 4.04 (d, J = 8.9 Hz, 1 H), 4.34 (d, J = 5.8 Hz, 2 H), 6.40−6.51 (m, 1 H), 6.73 (d, J =

16 Hz, 1 H), 7.01 (d, J = 8.7 Hz, 2 H), 7.25−7.50 (d, 7 H), 7.79 (s, 1 H), 8.54 (brs, 1 H); HRMS exact mass of $(M + Na)^+$, 578.1971 amu; observed mass of $(M + Na)^+$, 578.1966 amu.

(*Z*)-4-[2-({4-[(2,4-Dioxothiazolidin-5-ylidene)methyl]phenoxy}-methyl)-2,5,7,8-tetramethylchroman-6-yloxy]-4-oxobutanoic Acid (5): ^{1}H NMR ($CDCl_3$) δ 1.36 (s, 3 H), 1.81−2.10 (m, 11 H), 2.62 (m, 2 H), 2.77−2.82 (m, 2 H), 2.88−2.92 (m, 2 H), 3.95 (d, J = 9.2, 1 H,), 4.02 (d, J = 9.2 Hz, 1 H), 6.96 (d, J = 6.6 Hz, 2 H), 7.40 (d, J = 6.6 Hz, 2 H), 7.77 (s, 1 H), 8.43 (brs, 1 H); HRMS exact mass of $(M + Na)^+$, 562.1506 amu; observed mass of $(M + Na)^+$, 562.1480.

(*Z*)-5-{3-[(6-Allyloxy-2,5,7,8-tetramethylchroman-2-yl)methoxy]-benzylidene}thiazolidine-2,4-dione (6): ^{1}H NMR ($CDCl_3$) δ 1.35 (s, 3 H), 1.75−1.98 (m, 1 H), 2.04−2.22 (m, 10 H), 2.61 (t, J = 5.9 Hz, 2 H), 3.95 (m, 2 H), 4.15 (d, J = 11.5 Hz, 2 H), 5.25 (d, J = 8.6 Hz, 1 H), 5.43 (d, J = 14.3 Hz, 1 H), 6.02−6.17 (m, 1 H), 7.01 (m, 2 H), 7.08 (m, 1 H), 7.35 (t, J = 6.9 Hz, 1 H), 7.75 (s, 1 H), 8.38 (s, 1 H); HRMS exact mass of $(M + Na)^+$, 502.1659 amu; observed mass of $(M + Na)^+$, 502.1677.

(*Z*)-5-{4-[(6-Allyloxy-2,5,7,8-tetramethylchroman-2-yl)methoxy]-3-bromobenzylidene}thiazolidine-2,4-dione (7): ^{1}H NMR ($CDCl_3$) δ 1.47 (s, 3 H), 1.94−2.19 (m, 11 H), 2.60−2.64 (m, 2 H), 4.00 (d, J = 9.2 Hz, 1 H), 4.07 (d, J = 9.2 Hz, 1 H), 4.16 (d, J = 5.5 Hz, 2 H), 5.23 (d, J = 10.4 Hz, 1 H), 5.41 (d, J = 17.2 Hz, 1 H), 5.98−6.11 (m, 1 H), 6.96 (d, J = 8.7 Hz, 1 H), 7.36 (dd, J = 8.7, 2.1 Hz, 1 H), 7.67 (d, J = 2.1 Hz, 1 H), 7.70 (s, 1 H), 8.30 (brs, 1 H); HRMS exact mass of $(M + Na)^+$, 580.0763 amu; observed mass of $(M + Na)^+$, 580.0763 amu.

(*Z*)-5-{4-[(6-Allyloxy-2,5,7,8-tetramethylchroman-2-yl)methoxy]-3-methoxybenzylidene}thiazolidine-2,4-dione (8): ^{1}H NMR ($CDCl_3$) δ 1.42 (s, 3 H), 1.88−1.92 (m, 1 H), 2.04−2.18 (m, 10 H), 2.61 (t, J = 7.2 Hz, 2 H), 3.88 (s, 3 H), 3.98 (d, J = 9.9 Hz, 1 H), 4.09 (d, J = 9.9 Hz, 1 H), 4.16 (d, J = 5.5 Hz, 2 H), 5.23 (d, J = 10.4 Hz, 1 H), 5.40 (d, J = 17.2 Hz, 1 H), 6.03−6.15 (m, 1 H), 6.96−7.06 (m, 3 H), 7.76 (s, 1 H), 8.34 (s, 1 H); HRMS exact mass of $(M + Na)^+$, 532.1764 amu; observed mass of $(M + Na)^+$, 532.1762 amu. Anal. ($C_{28}H_{31}NO_6S$) C, H, N.

(*Z*)-5-{4-[(6-Allyloxy-2,5,7,8-tetramethylchroman-2-yl)methoxy]-3-methylbenzylidene}thiazolidine-2,4-dione (9): ^{1}H NMR ($CDCl_3$) δ 1.43 (s, 3 H), 1.89−1.94 (m, 1 H), 2.05−2.20 (m, 10 H), 2.26 (s, 3 H), 2.61 (t, J = 6.5 Hz, 2 H), 3.95 (d, J = 9.3 Hz, 1 H), 4.02 (d, J = 9.3 Hz, 1 H), 4.16 (d, J = 5.5 Hz, 2 H), 5.23 (d, J = 10.4 Hz, 1 H), 5.41 (d, J = 17.3 Hz, 1 H), 6.04−6.15 (m, 1 H), 6.88 (d, J = 8.8 Hz, 1 H), 7.27 (s, 1 H), 7.29 (d, J = 8.0 Hz, 1 H), 7.76 (s, 1 H); HRMS exact mass of $(M + Na)^+$, 516.1815 amu; observed mass of $(M + Na)^+$, 516.1837 amu. Anal. ($C_{28}H_{31}NO_5S$) C, H, N.

(*Z*)-5-{4-[(6-Allyloxy-2,5,7,8-tetramethylchroman-2-yl)methoxy]-3-ethoxybenzylidene}thiazolidine-2,4-dione (10): ^{1}H NMR ($CDCl_3$) δ 1.45 (s, 3 H), 1.58 (s, 3 H), 1.85−1.95 (m, 1 H), 2.02 (s, 3 H), 2.12−2.25 (m, 7 H), 2.60 (m, 2 H), 3.97−4.31 (m, 6 H), 5.23 (d, J = 8.6 Hz, 1 H), 5.40 (d, J = 13.3 Hz, 1 H), 6.05−6.16 (m, 1 H), 6.94−7.10 (m, 3 H), 7.76 (s, 1 H), 8.31 (s, 1 H); HRMS exact mass of $(M + Na)^+$, 546.1921 amu; observed mass of $(M + Na)^+$, 546.1907 amu.

(*Z*)-5-(3-Fluoro-4-{[2,5,7,8-tetramethyl-6-(3-methylbut-2-enyloxy)chroman-2-yl]methoxy}benzylidene)thiazolidine-2,4-dione (11): ^{1}H NMR ($CDCl_3$) δ 1.42 (s, 3 H), 1.69 (s, 3 H), 1.78 (s, 3 H), 1.87−1.93 (m, 1 H), 1.96 (s, 3 H), 2.01−2.17 (m, 7 H), 2.61 (t, J = 6.5 Hz, 2 H), 4.02 (d, J = 9.5 Hz, 1 H), 4.10 (d, J = 9.5 Hz, 1 H), 4.15 (d, J = 7.2 Hz, 2 H), 5.57 (t, J = 6.9 Hz, 1 H), 7.05 (t, J = 8.3 Hz, 1 H), 7.17−7.23 (m, 2 H), 7.72 (s,1 H), 8.46 (brs, 1 H); HRMS exact mass of $(M + Na)^+$, 548.1877 amu; observed mass of $(M + Na)^+$, 548.1889 amu.

(*Z*)-5-(3-Bromo-4-{[2,5,7,8-tetramethyl-6-(3-methylbut-2-enyloxy)chroman-2-yl)methoxy]benzylidene}thiazolidine-2,4-dione (12): ^{1}H NMR ($CDCl_3$) δ 1.40 (s, 3 H), 1.69 (s, 3 H), 1.78 (s, 3 H), 1.91−1.97 (m, 1 H), 2.02−2.21 (m, 10 H), 2.61 (m, 2 H), 3.94 (d, J = 9.5 Hz, 1H), 4.03 (d, J = 9.5 Hz, 1 H), 4.14 (d, J = 6.8 Hz, 2 H), 5.58 (t, J = 7.1 Hz, 1 H), 6.96 (d, J = 8.6 Hz, 1 H), 7.38 (dd, J = 8.6, 2.0 Hz, 1 H), 7.67 (d, J = 2.0 Hz, 1 H), 7.79 (s,1 H), 8.56 (brs, 1 H); HRMS exact mass of $(M + Na)^+$, 608.1076 amu; observed mass of $(M + Na)^+$, 608.1094 amu. Anal. ($C_{29}H_{32}BrNO_5S$) C, H, N.

(*Z*)-5-(3-Methoxy-4-{[2,5,7,8-tetramethyl-6-(3-methylbut-2-enyloxy)chroman-2-yl]methoxy}benzylidene)thiazolidine-2,4-dione (13): ^{1}H NMR ($CDCl_3$) δ 1.42 (s, 3 H), 1.69 (s, 3 H), 1.78 (s, 3 H), 1.86−1.93 (m, 1 H), 2.01−2.17 (m, 10 H), 2.61 (t, J = 6.8 Hz, 2 H), 3.87 (s, 3 H), 4.00 (d, J = 9.5 Hz, 1 H), 4.09 (d, J = 9.5 Hz, 1 H), 4.14 (d, J = 6.8 Hz, 2 H), 5.58 (t, J = 7.1 Hz, 1 H), 6.96−7.06 (m, 3 H), 7.76 (s, 1 H); HRMS exact mass of $(M + Na)^+$, 560.2077; observed mass of $(M + Na)^+$, 560.2086.

(*Z*)-5-(3-Methyl-4-{[2,5,7,8-tetramethyl-6-(3-methylbut-2-enyloxy)chroman-2-yl]methoxy}benzylidene)thiazolidine-2,4-dione (14): ^{1}H NMR ($CDCl_3$) δ 1.44 (s, 3 H), 1.69 (s, 3 H), 1.78 (s, 3 H), 1.86−1.94 (m, 1 H), 2.02−2.20 (m, 10 H), 2.26 (s, 3 H), 2.61 (t, J = 3.2 Hz, 2 H), 3.95 (d, J = 9.3 Hz, 1 H), 4.03 (d, J = 9.3 Hz, 1 H), 4.17 (d, J = 6.9 Hz, 2 H), 5.58 (t, J = 5.5 Hz, 1 H), 6.88 (d, J = 9.2 Hz, 1H), 7.27 (s, 1 H), 7.29 (d, J = 9.2 Hz, 1H), 7.76 (s, 1 H), 8.24 (brs,1 H); HRMS exact mass of $(M + Na)$, 544.2128 amu; observed mass of $(M + Na)^+$, 544.2134 amu.

(*Z*)-5-(3-Ethoxy-4-{[2,5,7,8-tetramethyl-6-(3-methylbut-2-enyloxy)chroman-2-yl]methoxy)benzylidene}thiazolidine-2,4-dione (15): ^{1}H NMR ($CDCl_3$) δ 1.40−1.46 (m, 6 H), 1.70 (s, 3 H), 1.79 (s, 3 H), 1.87−1.93 (m, 1 H), 2.01 (s, 3 H), 2.09−2.17 (m, 7 H), 2.62 (t, J = 7.0 Hz, 2 H), 3.97−4.16 (m, 6 H), 5.58 (t, J = 7.1 Hz, 1 H), 6.97−7.08 (m, 3 H), 7.76 (s, 1 H), 8.59 (s, 1 H); HRMS exact mass of $(M + Na)$, 574.2342; observed mass of $(M + Na)^+$, 574.2122.

(*Z*)-5-[(4′-Fluoro-6-{[2,5,7,8-tetramethyl-6-(3-methylbut-2-enyloxy)chroman-2-yl]methoxy}biphenyl-3-yl)methylene]thiazolidine-2,4-dione (16): ^{1}H NMR ($CDCl_3$) δ 1.27 (s, 3 H), 1.69−1.94 (m, 8 H), 2.00 (s, 3 H), 2.10 (s, 3 H), 2.17 (s, 3 H), 2.46−2.61 (m, 2 H), 3.99 (s, 2 H), 4.14 (d, J = 7.0 Hz, 2 H), 5.58 (t, J = 7.1 Hz, 1 H), 7.02−7.10 (m, 3 H), 7.41−7.52 (m, 4 H), 7.81 (s, 1 H), 8.30 (brs, 1 H); HRMS exact mass of $(M + Na)^+$, 624.2190; observed mass of $(M + Na)^+$, 624.2206.

(*Z*)-5-{4-[2-(6-Butoxy-2,5,7,8-tetramethyl-chroman-2-yl)ethyl]-3-trifluoromethylbenzylidene}thiazolidine-2,4-dione (17): ^{1}H NMR ($CDCl_3$) δ 0.93 (t, J = 7.0 Hz, 3 H), 1.31−1.54 (m, 5 H), 1.73−1.84 (m, 2 H), 1.87−1.95 (m, 1 H), 1.95−2.19 (m, 10 H), 2.60 (m, 2 H), 3.62 (t, J = 6.7 Hz, 2 H), 4.03 (q, J = 9.0 Hz, 1 H), 4.08 (q, J = 9.3 Hz, 1 H), 7.09 (d, J = 9.0 Hz, 1 H), 7.59 (dd, J = 9.0, 2.1 Hz, 1 H), 7.70 (d, J = 2.1 Hz, 1H), 7.79 (s, 1 H), 8.83 (s, 1 H); HRMS exact mass of $(M + Na)^+$, 584.2058; observed mass of $(M + Na)^+$, 584.2094.

5-{4-[2-(6-Butoxy-2,5,7,8-tetramethylchroman-2-yl)ethyl]-3-trifluoromethylbenzyl}thaizolodine-2,4-dione (18): ^{1}H NMR ($CDCl_3$) δ 0.99 (t, J = 7.2, 3 H), 1,34−1.68 (m, 5 H), 1.69−1.86 (m, 2 H), 1.86−1.98 (m, 1 H), 1.98−2.22 (m, 10 H), 2.62 (1 H), 3.18 (m, 1 H), 3.46 (m, 1 H), 3.64 (t, J = 6.9 Hz, 2 H), 4.26 (q, J = 10 Hz, 2 H), 4.51 (m, 1 H), 6.95 (d, J = 6.6 Hz, 1H), 7.26 (d, J = 6.6 Hz, 1 H), 7.44 (s, 1 H), 8.165 (s, 1 H); HRMS exact mass of $(M + Na)^+$, 586.2215; observed mass of $(M + Na)^+$, 586.2237.

Cell Culture. ER-positive MCF-7 breast cancer cells were obtained from the American Type Culture Collection (Manassas, VA) and were maintained in DMEM/Ham's F-12 medium supplemented with 10% fetal bovine serum (FBS, Gibco) at 37 °C in a humidified incubator containing 5% CO_2.

Western Blot Analysis. MCF-7 cells were seeded in 10% FBS-containing DMEM/Ham's F-12 medium for 24 h and treated with various agents as indicated. After individual treatments for 24 h, both the incubation medium and adherent cells in T-25 or T-75 flasks were scraped and collected by centrifugation at 2200 rpm for 10 min. The supernatants were recovered, placed on ice, and triturated with 20−50 μL of a chilled lysis buffer (M-PER mammalian protein extraction reagent; Pierce, Rockford, IL), to which was added 1% protease inhibitor cocktail (set III, EMD Biosciences, Inc.; San Diego, CA). After a 30-min incubation on ice, the mixture was centrifuged at 16100*g* for 3 min. An amount of 2 μL of the suspension was taken for protein analysis using the Bradford assay kit (Bio-Rad, Hercules, CA). To the remaining solution was added the same volume of 2× SDS−polyacrylamide

gel electrophoresis sample loading buffer (100 mM Tris-HCl, pH 6.8, 4% SDS, 5% β-mercaptoethanol, 20% glycerol, and 0.1% bromphenol blue). The mixture was boiled for 10 min. Equal amounts of proteins were loaded onto 10% SDS−polyacrylamide gels. After electrophoresis, protein bands were transferred to nitrocellulose membranes in a semidry transfer cell. The transblotted membrane was blocked with Tris-buffered saline/0.1% Tween 20 (TBST) containing 5% nonfat milk for 90 min, and the membrane was incubated with the appropriate primary antibody in TBST/5% nonfat milk at 4 °C overnight. After being washed three times with TBST for a total of 45 min, the transblotted membrane was incubated with goat antirabbit or antimouse IgG-horseradish peroxidase conjugates (diluted 1:1000) for 1 h at room temperature and washed four times with TBST for a total of 1 h. The immunoblots were visualized by enhanced chemiluminescence.

Semiquantitative PCR Analysis of mRNA Transcripts of Cyclin D1 Gene. MCF-7 cells were subject to total RNA isolation by using the RNeasy minikit (Qiagen, Valencia, CA). RNA concentrations and quality were assessed spectrophotometrically by measuring absorption at 260 nm. Aliquots of 20 μg of total RNA from each sample were reverse-transcribed to cDNA using the Omniscript RT kit (Qiagen) according to manufacturer's instructions. The primers used were as follows: cyclin D1, forward, 5′-ATGGAACACCAGCTCCTGTGCTGC-3′, reverse, 5′-TCAGATGTCCACGTCCCGCACGT-3′, β-actin, forward, 5′-TCTACAATGAGCTGCGTGTG-3′, reverse, 5′-GGTCAGGATCTTCATGAGGT-3′. The reaction conditions were as follows: for cyclin D1, (1) initial denaturation at 95 °C for 5 min, (2) 34 cycles of amplification (95 °C for 1 min, 65 °C for 1 min 45 s, and 72 °C for 1 min), and (3) a final extension step of 10 min at 72 °C; for β-actin, (1) initial denaturation at 95 °C for 3 min, (2) 40 cycles of amplification (95 °C for 30 s, 58 °C for 20 s, and 72 °C for 45 s), and (3) a final extension step of 10 min at 72 °C. The PCR reaction products were separated electrophoretically in a 1.2% agarose gel and stained with ethidium bromide.

Cell Viability Analysis. The effect of individual test agents on cell viability was assessed by using the MTT assay in six replicates. Cells were seeded and incubated in 96-well, flat-bottomed plates in DMEM/Ham's F-12 medium with 10% FBS for 24 h and were exposed to various concentrations of test agents dissolved in DMSO (final DMSO concentration, 0.1%) in 5% FBS-supplemented DMEM/Ham's F-12 medium. Controls received DMSO vehicle at a concentration equal to that of drug-treated cells. The medium was removed and replaced by 200 μL of 0.5 mM MTT in 10% FBS-containing RPMI 1640 medium, and cells were incubated in the 5% CO_2 incubator at 37 °C for 2 h. Supernatants were removed from the wells, and the reduced MTT dye was solubilized in 200 μL/well DMSO. Absorbance at 570 nm was determined on a plate reader.

Acknowledgment. This work is supported by National Institutes of Health Grants CA-94829 and CA112250.

Supporting Information Available: Elemental analysis data. This material is available free of charge via the Internet at http://pubs.acs.org.

References

(1) Weinstein, I. B. Disorders in cell circuitry during multistage carcinogenesis: the role of homeostasis. *Carcinogenesis* **2000**, *21*, 857−864.
(2) Chung, D. C. Cyclin D1 in human neuroendocrine: tumorigenesis. *Ann. N. Y. Acad. Sci.* **2004**, *1014*, 209−217.
(3) Diehl, J. A. Cycling to cancer with cyclin D1. *Cancer Biol. Ther.* **2002**, *1*, 226−231.
(4) Stacey, D. W. Cyclin D1 serves as a cell cycle regulatory switch in actively proliferating cells. *Curr. Opin. Cell Biol.* **2003**, *15*, 158−163.
(5) Wang, C.; Li, Z.; Fu, M.; Bouras, T.; Pestell, R. G. Signal transduction mediated by cyclin D1: from mitogens to cell proliferation: a molecular target with therapeutic potential. *Cancer Treat. Res.* **2004**, *119*, 217−237.
(6) Fu, M.; Wang, C.; Li, Z.; Sakamaki, T.; Pestell, R. G. Minireview. Cyclin D1: normal and abnormal functions. *Endocrinology* **2004**, *145*, 5439−5447.
(7) Ewen, M. E.; Lamb, J. The activities of cyclin D1 that drive tumorigenesis. *Trends Mol. Med.* **2004**, *10*, 158−162.
(8) Zhou, P.; Jiang, W.; Zhang, Y. J.; Kahn, S. M.; Schieren, I.; Santella, R. M.; Weinstein, I. B. Antisense to cyclin D1 inhibits growth and reverses the transformed phenotype of human esophageal cancer cells. *Oncogene* **1995**, *11*, 571−580.
(9) Schrump, D. S.; Chen, A.; Consoli, U. Inhibition of lung cancer proliferation by antisense cyclin D. *Cancer Gene Ther.* **1996**, *3*, 131−135.
(10) Arber, N.; Doki, Y.; Han, E. K.; Sgambato, A.; Zhou, P.; Kim, N. H.; Delohery, T.; Klein, M. G.; Holt, P. R.; Weinstein, I. B. Antisense to cyclin D1 inhibits the growth and tumorigenicity of human colon cancer cells. *Cancer Res.* **1997**, *57*, 1569−1574.
(11) Kornmann, M.; Arber, N.; Korc, M. Inhibition of basal and mitogen-stimulated pancreatic cancer cell growth by cyclin D1 antisense is associated with loss of tumorigenicity and potentiation of cytotoxicity to cisplatinum. *J. Clin. Invest.* **1998**, *101*, 344−352.
(12) Saikawa, Y.; Kubota, T.; Maeda, S.; Otani, Y.; Kumai, K.; Kitajima, M. Inhibition of DNA methyltransferase by antisense oligodeoxynucleotide modifies cell characteristics in gastric cancer cell lines. *Oncol. Rep.* **2004**, *12*, 527−531.
(13) Chen, B.; Zhang, X. Y.; Zhang, Y. J.; Zhou, P.; Gu, Y.; Fan, D. M. Antisense to cyclin D1 reverses the transformed phenotype of human gastric cancer cells. *World J. Gastroenterol.* **1999**, *5*, 18−21.
(14) Sauter, E. R.; Yeo, U. C.; von Stemm, A.; Zhu, W.; Litwin, S.; Tichansky, D. S.; Pistritto, G.; Nesbit, M.; Pinkel, D.; Herlyn, M.; Bastian, B. C. Cyclin D1 is a candidate oncogene in cutaneous melanoma. *Cancer Res.* **2002**, *62*, 3200−3206.
(15) Sauter, E. R.; Herlyn, M.; Liu, S. C.; Litwin, S.; Ridge, J. A. Prolonged response to antisense cyclin D1 in a human squamous cancer xenograft model. *Clin. Cancer Res.* **2000**, *6*, 654−660.
(16) Weinstein, I. B. Cancer. Addiction to oncogenes, the Achilles heel of cancer. *Science* **2002**, *297*, 63−64.
(17) Huang, J. W.; Shiau, C. W.; Yang, Y. T.; Kulp, S. K.; Chen, K. F.; Brueggemeier, R. W.; Shapiro, C. L.; Chen, C. S. Peroxisome proliferator-activated receptor gamma-independent ablation of cyclin D1 by thiazolidinediones and their derivatives in breast cancer cells. *Mol. Pharmacol.* **2005**, *67*, 1342−1348.

JM060057H